Performance Characteristics of a Concentric Annular Heat Pipe: Part I—Experimental Prediction and Analysis of the Capillary Limit

A. Faghri
Professor.

S. Thomas
Graduate Research Assistant.

Mechanical Systems Engineering,
Wright State University,
Dayton, OH 45435

This paper describes the design, testing, and theoretical capillary limit prediction of a new heat pipe configuration, which is the concentric annular heat pipe. The concentric annular heat pipe is made of two concentric pipes of unequal diameters that create an annular vapor space. With this arrangement, capillary wicks can be placed on both the inside of the outer pipe and the outside of the inner pipe. This design significantly increases the heat capacity per unit length compared to conventional heat pipes, since the cross-sectional area of the wick as well as the surface area for heating and cooling are increased. The heat pipe was tested for the temperature distribution in the three sections of the heat pipe under various tilt angles and heating loads through the inner and outer pipes in the evaporator section. A simple analysis for the prediction of the capillary limitation of the concentric annular heat pipe is presented.

Introduction

Since the invention of the heat pipe by Grover et al. (1964) 25 years ago, much study has been done in the areas of heat pipe operation, factors limiting heat pipe performance, heat pipe applications, and design modifications for the improvement of the performance of heat pipes.

Because of the simplicity of design and ease of manufacture and maintenance, heat pipes have found applications in a wide variety of areas (Dunn and Reay, 1982; Chi, 1976) including energy conversion systems, cooling of nuclear reactors, cooling of electronic equipment, and high-performance space applications. The performance of a heat pipe often is critical and is judged in part by the amount of heat a unit length of the heat pipe can transport.

The need for an increase in the performance has led to intensive studies into the performance limitations of heat pipes and has spawned new designs ranging from complex chamber configurations to sophisticated composite capillary wick structures (Oshima, 1984). The new design proposed here is as simple as the original heat pipe design, and at the same time is expected to increase the heat transport capacity significantly.

The concentric annular heat pipe, as shown in Fig. 1, consists of two concentric pipes of unequal diameters attached by means of end caps, which create an annular vapor space between the two pipes. Wick structures are placed on both the inner surface of the outer pipe and the outer surface of the inner pipe. The space inside the inner pipe is open to the surroundings. An increase in performance is expected as a result of the increase in surface area exposed for the transfer of heat into and out of the pipe, and the increase in the cross-sectional area of the wick inside the pipe.

A significant limitation in any heat pipe design is that imposed by the performance of the wick. A specific capillary force is available in the heat pipe based on the type of wick used and the cross-sectional area of wick material available to transport liquid back to the evaporator section. As the heat rate into the pipe increases, the evaporation rate of fluid in the evaporator section also increases, which places a greater demand on the wick structure to pump the condensed liquid in the condenser section to the evaporator section. When the wick can no longer supply liquid to the evaporator section at a rate equal to the rate of evaporation occurring in that section, the capillary limit for that heat pipe has been reached. The result is that the liquid in the wick does not completely wet the evaporator section due to the liquid evaporating prematurely, which is called evaporator section dryout. The temperature of the evaporator section then increases dramatically to dangerous levels, until it is no longer safe to operate the heat pipe. By placing wick material on both internal walls of the concentric annular heat pipe, nearly twice as much wick cross-sectional area is available to pump condensate. Hence the capillary limit of the new heat pipe is expected to be significantly increased.

The exposed surface area available for heat input and output is important to the performance of heat pipes. Conventional heat pipe designs are limited in exposed surface area to that area on the outside of the pipe; thus radial heat flux occurs only through that surface. The annular heat pipe utilizes the exposed surface of the outer and inner pipes to increase the total radial heat flux. It is expected that this increase in exposed surface area per unit length of pipe will result in a large increase in the heat transport capacity of the pipe.

Several advantages of the concentric annular heat pipe are

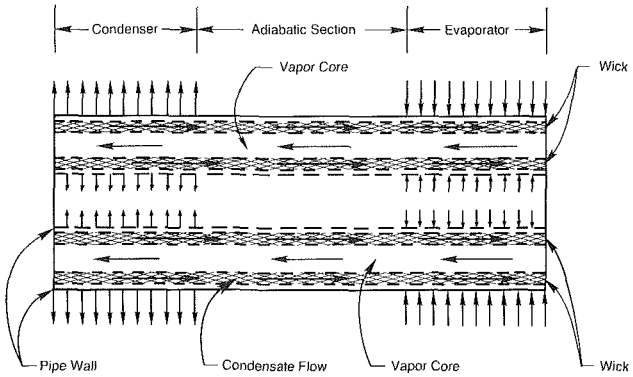

Fig. 1 Concentric annular heat pipe

Contributed by the Heat Transfer Division and presented at the National Heat Transfer Conference, Houston, Texas, July 1988. Manuscript received by the Heat Transfer Division May 4, 1988. Keywords: Heat Pipes and Thermosyphons.

apparent. First, the heat transport per unit length of this design will be more than that of the original heat pipe design. In many applications space is at a premium, so any increase in the heat transport for a given pipe size is significant. Second, since this design, like the original heat pipe design, is not specific to any working fluid, wick structure, or container material, many of the existing methods used to create high-capacity heat pipes can be used in conjunction with the concentric annular design. Certainly for high-power performance one can utilize any high-performance composite capillary wick structure. Finally, the annular heat pipe will be as easy to manufacture as a standard heat pipe, requiring no expensive tooling or other treatment. By this simple change in heat pipe design a large increase in performance with a minimum amount of sophistication has been achieved, making heat pipes more economical to build and use. A way that the concentric annular heat pipe could be used deals with applications that require exceptionally long heat pipes. Presently, when a very long heat pipe is needed the manufacturer builds several smaller heat pipes and ties these pipes together side-by-side and insulates where they are joined. This method is used because of the limitation of the capillary wick over long distances. Instead of tying the pipes together side-by-side where the area of contact between the pipes is minimal, a concentric annular heat pipe could be used to join the two pipes by sliding the end of each pipe into the inner pipe of the annular heat pipe. This method would increase the area of contact significantly, which would increase the heat transfer capability of the extended heat pipe.

Analysis of the Capillary Limitation of the Concentric Annular Heat Pipe

In this section a simple analysis for predicting the capillary heat transport limitation of the concentric annular heat pipe will be presented. This is done to show the improvement of the heat transport capability of the new design over a conventional heat pipe with the same outer dimensions. This comparison is valid because the same assumptions were made for the prediction of the capillary limit of the conventional heat pipe.

Consider an annular heat pipe as shown in Fig. 1 when operating under steady-state conditions. The sum of the pressure changes in the closed-cycle system may be described by the following mathematical relation:

$$2[P_v(z_{\text{ref}})-P_v(z)]+[P_v(z)-P_{L,I}(z)]+[P_v(z)-P_{L,O}(z)] \quad (1)$$
$$+[P_{L,I}(z)-P_{L,I}(z_{\text{ref}})]+[P_{L,I}(z_{\text{ref}})-P_v(z_{\text{ref}})]$$
$$+[P_{L,O}(z_{\text{ref}})-P_v(z_{\text{ref}})]+[P_{L,O}(z)-P_{L,O}(z_{\text{ref}})]=0$$

Introducing into the above equation the capillary pressure P_C, defined as the pressure at the vapor side of the liquid interface minus that of the liquid side, results in

$$P_{C,I}(z)+P_{C,O}(z)=P_{C,I}(z_{\text{ref}})+P_{C,O}(z_{\text{ref}})+2\Delta P_v(z-z_{\text{ref}}) \quad (2)$$
$$+\Delta P_{L,I}(z_{\text{ref}}-z)+\Delta P_{L,O}(z_{\text{ref}}-z)$$

where in general the notation $\Delta P(z-z_{\text{ref}})$ means that ΔP is evaluated over the distance $(z-z_{\text{ref}})$.

Assuming that the z_{ref} is such that it is located at $z_{\min}$ where the capillary pressure is minimum and equal to zero results in the following equation:

$$P_{C,I}(z)+P_{C,O}(z)=2\Delta P_v(z-z_{\min})+\Delta P_{L,I}(z_{\min}-z) \quad (3)$$
$$+\Delta P_{L,O}(z_{\min}-z)$$

In conventional heat pipes, there exists a maximum capillary pressure that can be developed for a liquid-wick pair. However, for the concentric annular heat pipe there exist two different maximum capillary pressure forces for the inner and outer tubes. If a heat pipe is to operate continuously without drying out the wick, the required capillary pressure for each wall should not exceed the maximum possible capillary pressure. The magnitude of the capillary pressure may be determined by balancing the forces at the liquid-vapor interface. This requires that the maximum capillary pressure for each wall should be:

$$P_{C,\max,I}=\frac{2\sigma}{r_{c,I}} \quad (4)$$

$$P_{C,\max,O}=\frac{2\sigma}{r_{c,O}}$$

where r_c is the effective capillary radius of the wick pores at the liquid-vapor interface. For axially grooved wicks, r_c is equal to the groove width as shown by Chi (1976).

Upon the assumption of laminar flow and incompressible fluid, and neglecting the inertia terms and the shear stress at the vapor-liquid interface in the conservation of momentum equation, one can get the following force balances for the liquid flow in the inner and outer wall grooves:

$$\frac{dP_{L,I}}{dz}=\frac{-4\tau_{L,I}}{D_{h,L,I}}\pm\rho_L g\sin\theta \quad (5)$$

$$\frac{dP_{L,O}}{dz}=\frac{-4\tau_{L,O}}{D_{h,L,O}}\pm\rho_L g\sin\theta \quad (6)$$

where τ_L is the viscous stress at the liquid-solid interface and $D_{h,L}$ is the hydraulic diameter for the wick and is equal to $4\,W\,\delta/(W+2\,\delta)$ for open rectangular grooves where δ is the groove depth and W is the groove width.

Equations (5) and (6) can be represented in terms of the local axial heat flux Q_I and Q_O for the inner and outer walls, respectively

Nomenclature

A = cross-sectional area
D = diameter
f = coefficient of friction
g = gravitational acceleration
h_{fg} = heat of vaporization
K = wick permeability
L = heat pipe length
$\dot{m}$ = mass flow rate
P = pressure
ΔP = pressure difference
Q = axial heat flux
r_c = effective capillary radius
Re = Reynolds number
t = wall thickness
ΔT = temperature difference
w = velocity
W = groove width
z = axial distance along the heat pipe
δ = groove depth
ϵ = porosity
θ = inclination angle
μ = viscosity
ν = kinematic viscosity
ρ = density
σ = surface tension
τ = shear stress

Subscripts

av = average
C = capillary
ea = evaporator and adiabatic
h = hydraulic
I = inner wall
L = liquid phase
max = maximum
min = minimum
O = outer wall
ref = reference
v = vapor phase
W = wick

$$\frac{dP_{L,I}}{dz} = -F_{L,I}Q_I \pm \rho_L g \sin\theta \tag{5a}$$

$$\frac{dP_{L,O}}{dz} = -F_{L,O}Q_O \pm \rho_L g \sin\theta \tag{6a}$$

The F functions are defined in the following way:

$$F_{L,I} = \frac{\nu_L}{K_I A_{W,I} h_{fg}} \tag{7}$$

$$F_{L,O} = \frac{\nu_L}{K_O A_{W,O} h_{fg}} \tag{8}$$

where K is the wick permeability, A_w the wick cross-sectional area, ϵ the porosity, f the friction coefficient, and Re_L the wick-liquid Reynolds number. These properties are defined by the following relationships:

$$\mathrm{Re}_{L,I} = \frac{D_{h,L,I} w_{L,I}}{\nu_L} \qquad \mathrm{Re}_{L,O} = \frac{D_{h,L,O} w_{L,O}}{\nu_L}$$

$$f_{L,I} = \frac{\tau_{L,I}}{\rho_L \dfrac{w_{L,I}^2}{2}} \qquad f_{L,O} = \frac{\tau_{L,O}}{\rho_L \dfrac{w_{L,O}^2}{2}} \tag{9}$$

$$Q_I = w_{L,I}\epsilon_I A_{W,I}\rho_L h_{fg} \qquad Q_O = w_{L,O}\epsilon_O A_{W,O}\rho_L h_{fg}$$

$$K_I = \frac{\epsilon_I D_{h,L,I}^2}{2(f_{L,I}\mathrm{Re}_{L,I})} \qquad K_O = \frac{\epsilon_O D_{h,L,O}^2}{2(f_{L,O}\mathrm{Re}_{L,O})}$$

The total local axial heat flux Q is the sum of the inner wall local axial heat flux Q_I and the outer wall local axial heat flux Q_O. Laminar incompressible fully developed fluid flow analysis in open rectangular passages shows that $f\cdot\mathrm{Re}$ is only a function of the geometry and dimensions of the wick. Therefore Q_I and Q_O are the only variables in equations (5*a*) and (6*a*) that change with axial distance along the heat pipe. The value of $f\cdot\mathrm{Re}$ needed for the evaluation of F can be obtained from Chi (1976) for the family of rectangular tubes as well as flow between concentric cylinders.

The problem of calculating the vapor pressure drop in the annulus is complicated in the evaporating and condensing regions by the radial vapor flow due to evaporation and condensation. It is convenient to neglect this effect of blowing and suction on the vapor pressure drop to obtain a closed-form solution. For a more accurate prediction one should use an analysis that includes the effect of blowing and suction on the vapor pressure drop as given by Faghri (1986) and Faghri and Parvani (1988). Upon the application of the conservation of axial momentum to the vapor flow between the concentric pipes, one obtains the following relationship provided that the flow is laminar:

$$A_v \frac{dP_v}{dz} = -\tau_{v,I}(\pi D_I) - \tau_{v,O}(\pi D_O) - A_v \frac{d\rho_v w_v^2}{dz} + (\dot{m}_I + \dot{m}_O) w_v \tag{10}$$

Since the mass flux of the vapor is related to the axial heat flux at the same z ($Q = \rho_v w_v A_v h_{fg}$), equation (10) can be presented in the following form when the last term on the right-hand side of the above equation is neglected:

$$\frac{dP_v}{dz} = -F_{v,av}Q - E_v \frac{dQ^2}{dz} \tag{11}$$

where

$$F_{v,av} = \frac{2(f_{v,av}\mathrm{Re}_v)\nu_v}{A_v D_{h,v}^2 h_{fg}}$$

$$f_{v,av} = \frac{\tau_{v,av}}{\rho_v w_v^2/2} = \frac{D_O\tau_{v,O} + D_I\tau_{v,I}}{(D_O + D_I)\rho_v w_v^2/2}$$

$$\mathrm{Re}_v = \frac{\rho_v w_v D_{h,v}}{\mu_v}$$

$$D_{h,v} = D_O - D_I$$

$$E_v = \frac{1}{A_v^2 \rho_v h_{fg}^2}$$

Substituting $\Delta P_L(z - z_{\min})$ and $\Delta P_v(z - z_{\min})$ from equations (5*a*), (6*a*), and (11) into equation (3) and neglecting the effect of gravity results in the following equation:

$$2\sigma\left(\frac{1}{r_{c,I}} + \frac{1}{r_{c,O}}\right) = 2F_{v,av}\int_0^L Q dz + \int_0^L (F_{L,I}Q_I + F_{L,O}Q_O) dz$$

The above relation simplifies, if one assumes that the geometry and dimensions of the grooves of the inner pipe are the same as the outer pipe, as well as the same heat input to the inner and outer walls, i.e., $F_{L,I} = F_{L,O} = F_{L,av}$ and $Q_I = Q_O = Q/2$.

$$\int_0^L Q dz = \frac{2\sigma\left(\dfrac{1}{r_{c,I}} + \dfrac{1}{r_{c,O}}\right)}{2F_{v,av} + F_{L,av}}$$

The maximum heat transport for a conventional heat pipe is given by the following equation:

$$\int_0^L Q dz = \frac{2\sigma/r_c}{F_L + F_v}$$

A comparison of the maximum heat transport capillary limit of the axially grooved concentric annular heat pipe proposed for experiment to a conventional heat pipe with the same outer diameter using the above analysis shows an increase of 80 percent using water as the working fluid at 100°C with the dimensions of the pipes and grooves as specified in Tables 1 and 2. The experimental prediction of the capillary limit indicated the same relative increase for this new design over the conventional heat pipe.

Experimental Apparatus and Procedure

Because the major objective of this project is to compare the performance of the concentric annular heat pipe to the performance of a conventional heat pipe of the same size, it was decided that two pipes should be built: a conventional heat pipe and a concentric annular heat pipe (see Tables 1 and 2, respectively). The pipes are of equal length and have the same external diameters. This allows a comparison of the performance per unit size. The two pipes are made of the same material and utilize the same working fluid. In order to observe the capillary pressure effect, the two pipes employ the same wick structure, although the concentric annular heat pipe has approximately twice the wick volume. With this criterion, it is hoped that a valid comparision can be made.

Summaries of the design parameters for the annular and the conventional heat pipe are given in Tables 1 and 2, respectively. It was decided that the wick structure to be used in the heat pipe would be axial grooves, which eliminated the need for a complicated wick installation procedure (Fig. 2).

The outer copper pipe to be used in the two heat pipes was commercially available, 973 mm in length and o.d. = 50 mm with 120 0.5 mm × 0.5 mm axial grooves extruded on the inner

Table 1 Design summary of the concentric annular heat pipe

Materials			
Outer pipe	Copper		
Inner pipe	Copper		
End caps	Copper		
Working Fluid	Water		
Dimensions			
Total Length	973 mm	Outer pipe	Inner pipe
Evaporator Length	300 mm	OD 50 mm	29.7 mm
Adiabatic Length	473 mm	ID 46.6 mm	25.4 mm
Condenser Length	200 mm	Tw 1.7 mm	2.15 mm
Grooves			
		Outer pipe	Inner pipe
Number		120	97
Width		0.5 mm	0.5 mm
Depth		0.5 mm	0.5 mm
Total groove volume	54.25 cc		
Fluid Inventory			
Quality	Distilled water		
Quantity	68 cc filled at 21°C		

Table 2 Design summary of conventional pipe

Materials		
Outer pipe	Copper	
End caps	Copper	
Working Fluid	Water	
Dimensions		
Total Length	973 mm	
Evaporator Length	300 mm	OD 50 mm
Adiabatic Length	473 mm	ID 46.6 mm
Condenser Length	200 mm	Tw 1.7 mm
Grooves		
Number	120	
Width	0.5 mm	
Depth	0.5 mm	
Total groove volume	30 cc	
Fluid Inventory		
Quality	Distilled water	
Quantity	41 cc filled at 21°C	

Table 3 Heater assembly design specifications

Dimensions	Inner Assembly	Outer Assembly
Length	300 mm	300 mm
OD	25.4 mm	---
ID	---	50.4 mm
Surface Area	15959.3 mm^2	32142.3 mm^2
Heating Element		
Length	2.24 m	2.38 m
Diameter	2.36 mm	4.77 mm
Voltage	220 v	220 v
Max. Power	1200 w	4800 w
Assembly Base		
Material	Aremcolox 502-600	
Length	300 mm	
OD	19.05 mm	
Thermocouples		
NBS Type	T (30 gauge)	T (28 gauge)
# of thermocouples	7	7

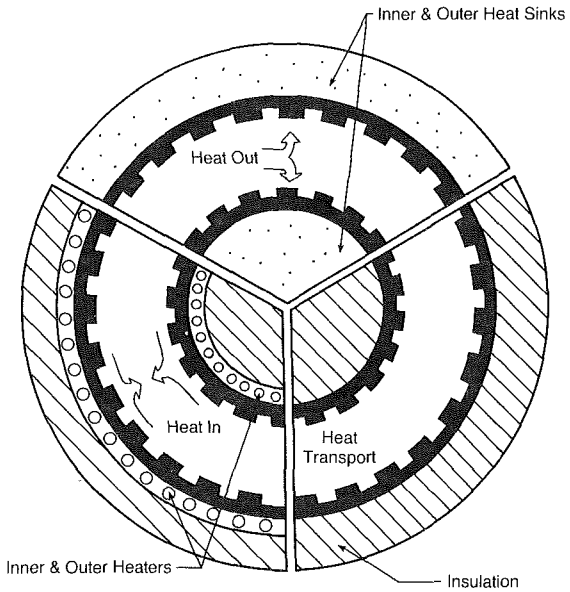

Fig. 2 Concentric annular heat pipe design concept

wall. The inner pipe for the annular heat pipe was machined from a copper tube with i.d. = 25.4 mm and o.d. = 29.7 mm. Ninety-seven 0.5 mm × 0.5 mm axial grooves were cut on the outer wall over the length of the pipe using a vertical milling machine with a precision saw cutter. The ends of each pipe were machined so that the end caps fit snugly into them.

All of the parts were carefully fabricated, cleaned, and deoxidized using the standard procedures suggested by Chi (1976), and the end caps were TIG welded to the tubes in an inert argon gas environment. A bellows-type valve was attached to the fill tube of the heat pipe to facilitate sealing, purging, and charging of the fluid inventory inside the heat pipe. A thermocouple probe was inserted through the condenser end cap a distance of 75 mm into the vapor core to measure the vapor temperature.

The heat pipes were processed in a specially built heat pipe filling station. The conventional and concentric annular heat pipes were evacuated to a vacuum on the order of 10^{-5} torr, and filled with 41 and 68 cc of degassed, distilled water at 21°C, respectively.

Heat was input to the concentric annular heat pipe by two heaters (see Table 3). The inner heater assembly was designed to slide into the inner pipe (i.d. = 25.4 mm) in the evaporator end of the concentric annular heat pipe. It consisted of a 2.24-m-long, 1200 W heater rod coiled around a core of insulating material 300 mm in length. This heater assembly was covered with thermally conductive cement so that its outer

diameter was o.d. = 25.2 mm. This allowed the completed inner heater assembly to slide into the inner pipe of the concentric annular heat pipe. Seven thermocouples were mounted on the outer surface of the heater assembly to measure the temperature of the inner wall of the heat pipe in the evaporator section.

The outer heater for the concentric annular heat pipe was a 4800-W heater rod of length 2.38 m and diameter 4.77 mm. The heater rod was tightly wrapped around the evaporator in a uniform spiral arrangement and was held in place with Sauereisen electric heater cement. This prevented the heater rod from expanding away from the heat pipe when the heater was operating. Seven thermocouples were mounted between the heater coils on the pipe wall to monitor the outer evaporator temperature. Each heater assembly was powered by its own 220-V variable a-c transformer, allowing the heat input to be varied from zero to the maximum wattage. The power input was monitored by a voltmeter and an ammeter connected to each variac and was checked with precision wattmeters.

The wall temperature of the adiabatic section of the concentric annular heat pipe was measured by thermocouples mounted on both the inner and outer walls. Seven thermocouples were mounted on a rod of insulating material (Aremcolox 502-600) of o.d. = 25.2 mm that was inserted into the inner pipe in the adiabatic section. Seven thermocouples were mounted directly onto the outer walls of the concentric annular heat pipe. A thermocouple was also mounted on each end cap of the heat pipe.

The condenser section of the concentric annular heat pipe has two heat sinks (see Table 4). The inner heat sink fits inside the inner pipe of the heat pipe. The outer heat sink fits over the outer pipe of the heat pipe. The inner heat sink (o.d. = 25.4 mm) has two end caps. One cap has two holes—one inlet and one outlet—and the other cap is solid. An inner baffle runs the length of the heat sink and has a hole in it at the end where the solid end cap is. This forces the coolant to travel the entire length of the heat sink, which ensures even cooling. The length of the inner heat sink is the length of the condenser section plus the length of each end cap. The total length is 219 mm. T-fittings were placed at the inlet and outlet of the inner heat sink to allow for the installation of thermocouples in the coolant stream with which the mixed-mean inlet and outlet temperatures were measured. Four axial grooves were cut on the outside of the inner heat sink to accommodate eight thermocouples, which were placed at regular intervals along the length of the heat sink. This allowed for the measurement of the temperature distribution on the inside of the inner pipe. These grooves are cut 6.35 mm wide × 1.59 mm deep and run the length of the heat sink.

The outer heat sink for the concentric annular heat pipe was 1/4 in. o.d. soft copper tubing, which was tightly wrapped around the condenser section and held in place with clamps at each end. The coils of tubing were wrapped around the pipe such that the coils were side-by-side. T-fittings were placed at the inlet and outlet of the outer heat sink to measure the inlet and outlet temperatures of the cooling water.

The outer heater for the conventional heat pipe was two heater rods of length 2.24 m and diameter 2.36 mm. Each heater rod was tightly wrapped around one-half of the length

Table 4 Heat sink design specifications

Dimensions	Inner Sink	Outer Sink
Length	219 mm	200 mm
OD	25.4 mm	63.5 mm
ID	---	50.4 mm
Surface Area	17475 mm^2	31667 mm^2
Material		
Outer pipe	Copper (tw = 1.27 mm)	1/4 in OD Copper tubing
Baffle	Copper	---
Working fluid	Water	Water
Thermocouples		
NBS Type	T (30 gauge)	
# of thermocouples	8	
Flow Meter		
Max. flow rate	906 ml/min.	1812 ml/min.
Min. flow rate	24 ml/min.	48 ml/min.
Fluid	Water	Water

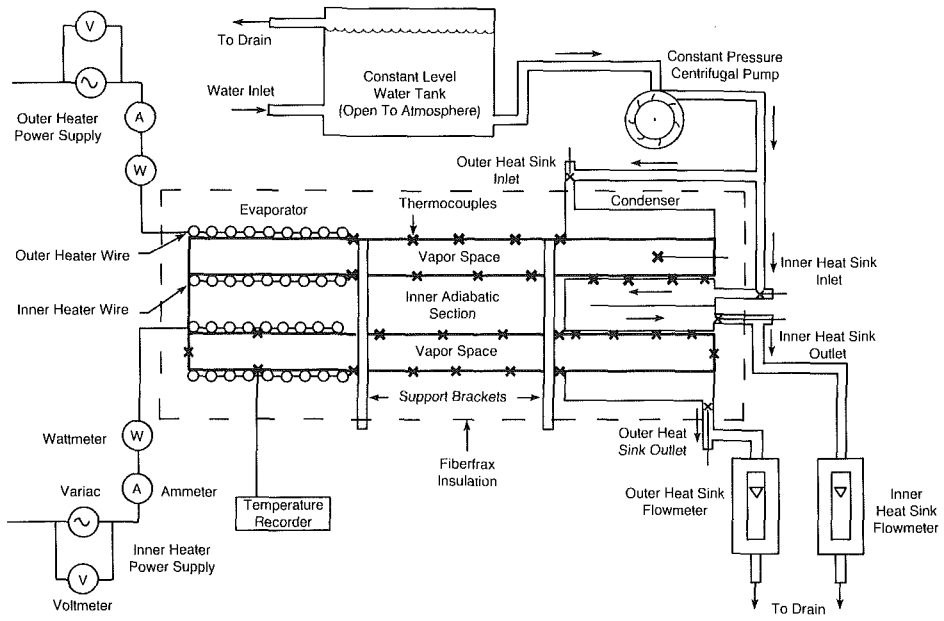

Fig. 3 Experimental setup

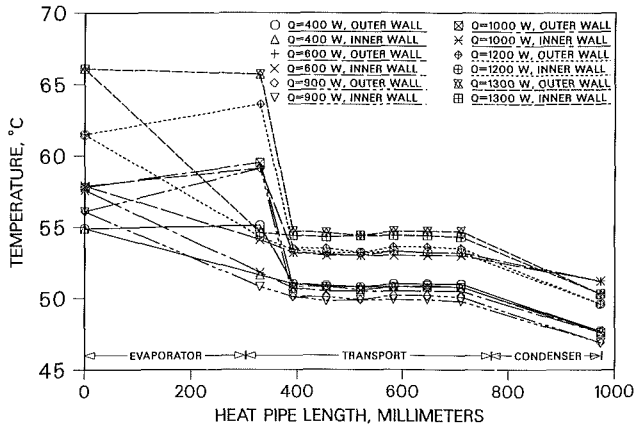

Fig. 4 Axial temperature profile for the concentric annular heat pipe

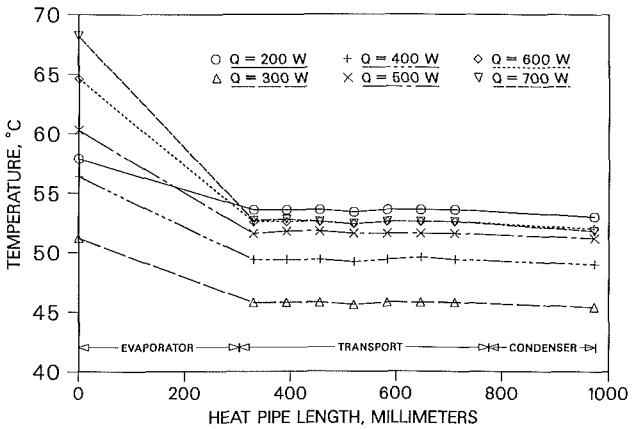

Fig. 5 Axial temperature profile for the conventional heat pipe

of the evaporator section with an even spiral pitch. The heaters were covered with electric heater cement and seven thermocouples were mounted between the coils on the pipe wall. When the conventional heat pipe was tested, the heat input through each heater was the same to ensure uniform heating.

The adiabatic section and the condenser section of the conventional heat pipe were identical with respect to the thermocouple instrumentation and the the heat sink as the outer adiabatic section and the outer condenser section of the annular heat pipe.

A schematic of the test setup is shown in Fig. 3. The heat pipes were mounted on a test stand with the required heater and heat sink assemblies installed complete with thermocouples. The thermocouples were attached to a monitoring device and variable area flow meters were installed at the outlet of the heat sinks to measure cooling water flow rates. Cooling water was supplied to the heat sinks by a centrifugal pump connected to a constant head reservoir in order to maintain constant pressure and therefore a steady coolant flow.

The entire length of the heat pipe assembly was insulated with 6 in. of "Fiberfrax" insulation material. The heat pipe was made parallel to the base of the test setup and the base was then mounted on leveling jacks. Using these jacks the heat pipe could be adjusted to any tilt angle desired.

Tests were performed to establish the maximum heat transport capacity of the heat pipe before wick dryout at negative (adverse) and zero tilt angles. The operating (adiabatic) temperature was held at $50°C \pm 5°C$ for all of the tests to ensure repeatability of the results. A thermocouple probe was used to compare the vapor temperature to adiabatic wall temperatures to confirm the absence of noncondensible gases in the condenser end of the heat pipe. Energy balances between the heat input by the heaters and the heat removed by the heat sinks were monitored, and flow rates through the heat sinks were maintained to ensure an energy balance of at least 90 percent. The criterion used to establish the maximum heat transport capacity was steady-state operating conditions with no evaporator dryout. Evaporator dryout was defined as that point when the temperature difference between the adiabatic section and the evaporator end cap was greater than 12°C. Type T thermocouples were used, which can be read with an uncertainty of $\pm 1/4$ percent. A standard error analysis technique was applied for the calculation of the heat rate Q, which yielded an uncertainty of ± 6 percent.

Results

Information was gathered from several test runs on each heat pipe and the data were combined to observe the overall performance of the concentric annular heat pipe with an emphasis on an increase in the heat transport capacity as compared to the conventional heat pipe. Figures 4 and 5 show the axial temperature profiles of the two pipes up to the maximum stable heat transport capacity. These graphs show that the concentric annular heat pipe performed nearly 82 percent better than the conventional heat pipe, showing a maximum stable operating limit of 1300 W as compared to 700 W for the conventional heat pipe.

The axial temperature profiles of the concentric annular heat pipe are shown in Fig. 4. In this graph, each power setting has the same line texture but the inner temperature profile has a different data point symbol than the outer temperature profile. For example, the first test is for a total heat input of 400 W. The inner temperature distribution for this setting is denoted by a solid line with triangles marking data points. The outer temperature profile for this same setting is shown by a solid line with octagons marking data points. Figure 4 shows clearly that the temperatures of the inner and outer adiabatic sections were isothermal and within 1°C of each other for all of the power settings.

The heat input in the inner wall evaporator is smaller than the outer wall evaporator due to smaller heater capacity in the inner wall in comparison to the outer heater in the present experiment as well as the possibility of boiling due to the smaller surface area. Upon combining the results of Figs. 4 and 8, one can see how the heat is distributed between the inner and outer walls.

Figure 5 shows the temperature distributions of the conventional heat pipe under various heat loads. The adiabatic temperatures for this pipe at all of the settings were also isothermal to within 1°C.

Adverse tilt tests were performed on the concentric annular heat pipe at tilt angles from -1 deg to 0 deg and the results are shown in Fig. 6. An adverse tilt is when the evaporator section is above the condenser section, which forces the condensate to be pumped uphill by the wick structure. Positive (favorable) tilt angle tests were not performed on the concentric annular heat pipe because the heater temperature in the inner evaporator section exceeded the maximum temperature recommended by the manufacturer of the thermocouples that were used in the inner heater section at powers above 1300 W. Figure 6 demonstrates that the maximum input power increases as the evaporator section is lowered with respect to the condenser section of the concentric annular heat pipe.

The heat transport rate versus the tilt angle for the conventional heat pipe is shown in Fig. 7. The maximum stable heat rate for the conventional heat pipe at 0 deg tilt was 700 W. This heat pipe displayed the same behavior in the tilt test as the concentric annular heat pipe.

The condenser heat output through the inner and outer pipe

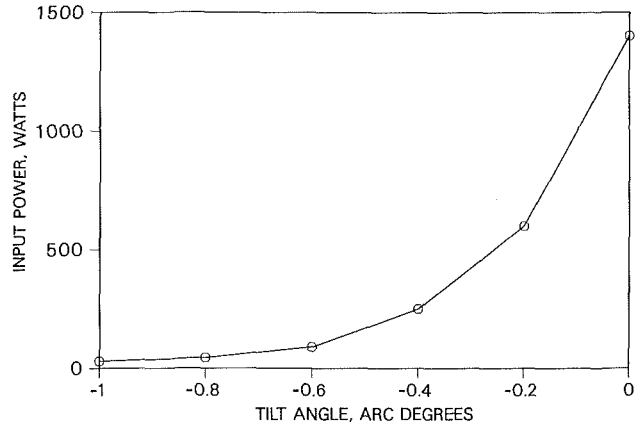

Fig. 6 Maximum input power versus tilt angle for the concentric annular heat pipe

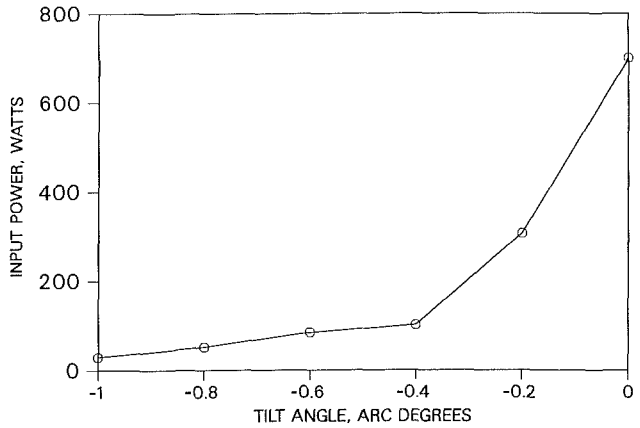

Fig. 7 Maximum input power versus tilt angle for the conventional heat pipe

walls versus the evaporator heat input through each pipe wall is presented in Fig. 8. This graph shows that the heat input through the inner pipe wall in the evaporator section is significantly smaller than the heat extracted from the inner pipe in the condenser section at all of the power settings. Likewise, the heat input through the outer pipe in the evaporator is greater than the heat taken away by the outer condenser. This means that all of the working fluid that condenses onto the inner pipe wall in the condenser section does not reach the inner evaporator section. This phenomenon is the result of communication of the working fluid between the inner and outer pipes. A meniscus is formed in the condenser section where the inner pipe and the end cap are joined, which allows part of the working fluid that condenses onto the inner pipe to drain down to the outer pipe. In future investigations this phenomenon should be prevented by proper wick and end cap design. This will increase the amount of heat that can be transferred by the inner pipe.

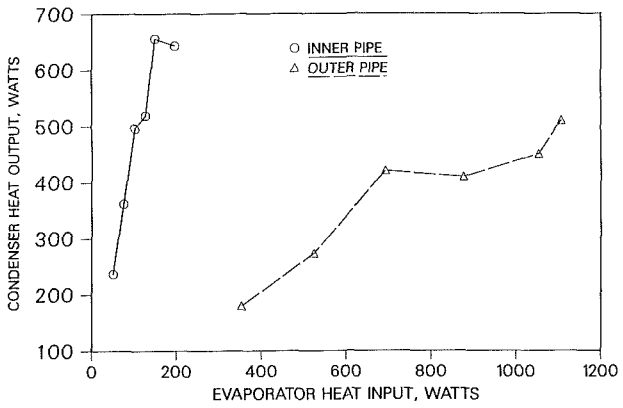

Fig. 8 Evaporator and condenser performance for the concentric annular heat pipe

Conclusions

A new heat pipe design called the concentric annular heat pipe has been developed and a 1-m-long copper–water prototype was fabricated and tested successfully. The design is simple to manufacture and can be used with any existing high-performance wick structure. This design shows a significant increase in the heat capacity per unit length compared to conventional heat pipes with the same outer diameter. The potential of the application of the new design in the heat exchange industry would be significant compared to conventional heat pipes due to size, geometry, and heat capacity performance. Furthermore, temperature uniformity in the inner and outer walls makes this device an ideal simplified temperature control device for furnace applications.

Acknowledgments

Funding for this work was provided by the Thermal Energy Group of the Aero Propulsion Laboratory of the U.S. Air Force under contract No. F-33615-81-C-2012. The authors are indebted to Dr. E. T. Mahefkey and Dr. J. E. Beam for their technical assistance during the project.

References

Chi, S. W., 1976, *Heat Pipe Theory and Practice*, Hemisphere Publishing Corporation, New York.

Dunn, P. D., and Reay, D. A., 1982, *Heat Pipes*, 3rd ed., Pergamon Press, New York.

Faghri, A., 1986, "Vapor Flow Analysis in a Double-Walled Concentric Heat Pipe," *Numerical Heat Transfer*, Vol. 10, pp. 583–595.

Faghri, A., and Parvani, S., 1988, "Numerical Analysis of Laminar Flow in a Double-Walled Annular Heat Pipe," *Journal of Thermophysics and Heat Transfer*, Vol. 2, No. 2, pp. 165–171.

Grover, G. M., Cotter, T. P., and Erikson, G. F., 1964, "Structures of Very High Thermal Conductance," *Journal of Applied Phys.*, Vol. 35, No. 6, pp. 1990–1991.

Oshima, K., 1984, *Research and Development of Heat Pipe Technology*, Japan Technology and Economics Center, Inc., Tokyo.